Designing Hollow-Fiber Contactors

Hollow-fiber contactors can provide fast mass transfer without flooding or loading. They are a promising alternative to packed towers for gas treating, and to centrifugal extractors for liquid-liquid extraction. Hollow-fiber contractors can be designed effectively using the mass transfer correlations reported in this paper. The correlations, based on aqueous deaeration and carbon dioxide absorption, are similar to earlier heat and mass transfer correlations, but can be complicated by diffusion across the fiber wall and by alterations in fiber geometry.

Ming-Chien Yang, E. L. Cussler
Department of Chemical Engineering
and Materials Science
University of Minnesota
Minneapolis, MN 55455

Hollow fibers can allow rapid mass transfer, much more rapid than that in conventional equipment. For example, acid gas treatment with hollow fibers can take place over ten times faster than that in packed towers (Zhang and Cussler, 1985a). Liquid-liquid extraction with hollow fibers can occur 100 times faster than in spray towers (Kiani et al., 1984; Kim, 1984a, b). The rates observed in extraction are comparable to those in centrifugal extractors, but they are achieved at a much lower equipment cost.

The objective of this paper is to report design equations for modules containing such hollow fibers. These equations reinforce earlier, less quantitative conclusions. They show that the mass transfer coefficients in these modules are not unusually large. However, the modules' surface area per volume is often very large—up to 40 cm^2/cm^3 (1,200 ft^2/ft^3). The modules also are not prey to the loading, flooding, and channeling that can compromise the performance of more conventional equipment (Treybal, 1980). Our results allow these potential advantages to be more exactly anticipated.

The chemical system chosen for most of our experiments is the removal of oxygen from water. This system has commercial value in the pretreatment of boiler feed water and in the deaeration of bottled beverages to improve shelf life. However, we chose it because oxygen does not chemically react with water and because oxygen concentrations are easily monitored using an oxygen-sensitive electrode. As a result, the system is uncomplicated by the chemical reactions basic to acid gas treatment and ammonia absorption (Astarita et al., 1983). This makes our analysis more certain. We have buttressed our conclusions for oxygen with additional experiments for carbon dioxide.

In the sections that follow, we first discuss the construction of the modules and the way in which we used them to study deaeration. We then report the results of experiments made with these modules, and describe the mechanism responsible for controlling the mass transfer in the various cases. Finally, we discuss the correlations that can be inferred from our experiments, and compare these with correlations previously reported for analogous heat and mass transfer problems. This discussion provides a basis for designing hollow-fiber membrane modules for contacting both gases and liquids in other situations.

The chief conclusion of these sections is that the key to hollow-fiber modules is the area per volume, which is much greater than that in conventional equipment. Thus the advantages of the modules reflect only the very high contact areas achieved under conditions that would commonly cause flooding or channelling. The key to hollow-fiber modules is not the mass transfer coefficient, which is about the same size as that in conventional equipment. This normal mass transfer coefficient is due to the lack of any membrane resistance. In other words, the membrane does not retard the mass transfer.

Experimental

Oxygen, nitrogen, and carbon dioxide (Matheson) were reagent grade and used as received. Sodium hydroxide used to analyze carbon dioxide concentrations was purchased as a 0.1M solution (Fisher) and diluted when necessary.

Hollow-fiber modules were made by potting the desired number of fibers into an external shell. The fibers were microporous polypropylene, of about 0.04 cm OD, and 0.003 cm wall thickness (Celgard, Celanese, Charlotte, N.C.). The pores, of about 300 Å dia., cover about 33% of the fiber surface. The potting compound was an epoxy (FE-9000, H. B. Fuller, St. Paul, MN). The shells were either glass or polymethylmethacrylate.

The three types of modules made differed largely in the geometry of the shell. In the first type, shown on the left in Figure 1, the shell was cylindrical, so that the finished module looked like a small shell-and-tube heat exchanger. Flows in modules like this commonly ranged from 2 to 20 cm^3/s. The second type, which is not shown, is similar, but has a rectangular cross section instead of a cylindrical one. In both the first and second types, flow outside the fibers was parallel to the fibers.

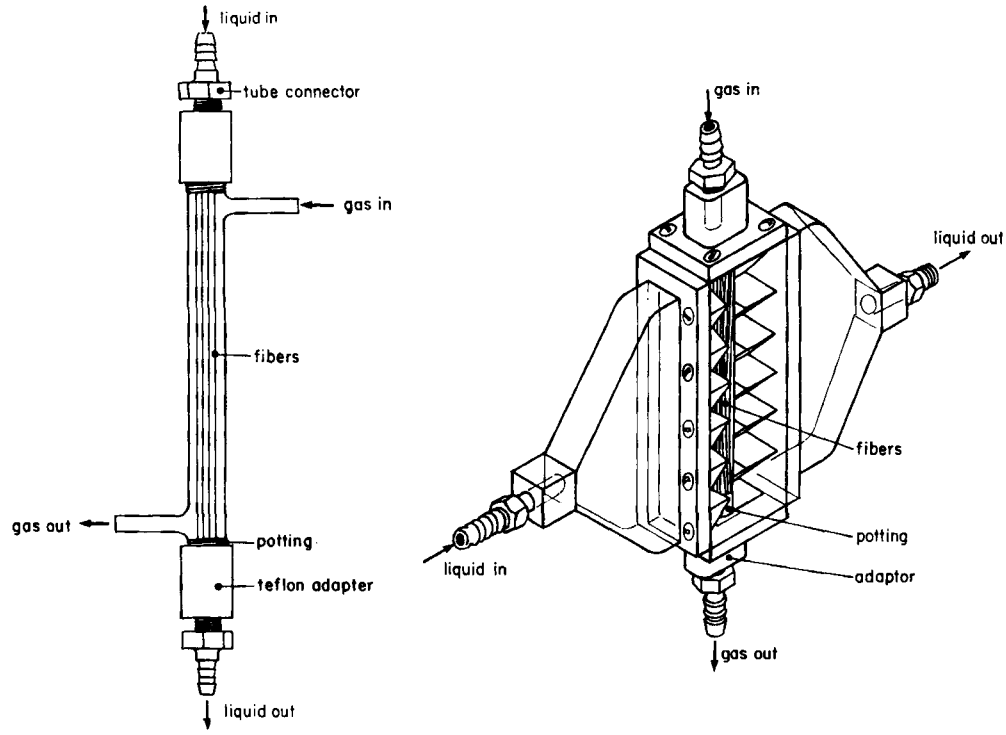

Figure 1. Hollow-fiber modules used in this work.

The third type of module, shown on the right in Figure 1, allows liquid cross flow of 2 to 50 cm^3/s outside of and perpendicular to the fibers. The fibers themselves lie across a rectangular channel. The two open faces of this channel are connected to the diverging and converging sections shown. The physical details of all three types of modules are given in Table 1.

These modules were used in the apparatus shown in Figure 2, details of which are given elsewhere (Yang, 1986). Sweep gas supplied from a gas cylinder flowed through the module and then was vented to the atmosphere. In some experiments, a vacuum was used instead of a sweep gas, with equivalent results. A rotameter (7641H, Matheson) was used to measure the gas flow rate. To maintain the pressure of the gas at 1 atm (101 kPa), the outlet tube was inserted in a beaker of water. The liquid was pumped from a reservoir by a metering pump (RP-D-2-CKC, Fluid Metering, Inc.) and monitored by a second identical rotameter. However, the liquid flow rate was determined as the time required to fill a fixed volume. The liquid can be pumped through either the shell side or the tube side (the lumen of the fibers) of the module. Downstream, liquid samples were collected in bottles, but only after initial transients ceased and the module was operating in steady state. The concentration of oxygen was determined by an oxygen electrode (97-08-00, Orion Research). The concentration of carbon dioxide was determined to within ±3% by titration of the remaining base, using phenolphthalein as the indicator (Snell and Hitton, 1966).

Table 1. Dimensions of Hollow-Fiber Modules

Type and Lable	No. of Fibers	Void Fraction in Shell† %	Length cm	Interfacial Area cm^2	Comments
Parallel Flow*					
PS16	16	97.5	6.4	13.3	Spaced regularly 1.5 mm apart
PM16	16	97.5	11.1	23.0	Well-spaced
PL16	16	97.5	21.3	44.2	Well-spaced
PM120	120	74	10.2	158.8	Close-packed
PM300	300	35	12.7	494.3	Highly close packed
Kobe	2,100	60	22.0	6,000.3	Highly close packed
Cross Flow**					
CM72	72	94	10	105.4	Well-spaced
CM750	750	36	10	1,098.0	Highly close packed

†All parallel flow modules except Kobe used tubes of 1.0 cm ID. Kobe module was a 1.2 cm × 8.2 cm rectangular channel. Cross flow modules were 1.0 cm × 10.0 cm cross section, 2.0 cm deep.

*These fibers had 0.0413 cm ID, 0.00265 cm wall thickness, and 0.33 void fraction.

**These fibers had 0.0466 cm OD, 0.00265 cm wall thickness, and 0.33 void fraction.

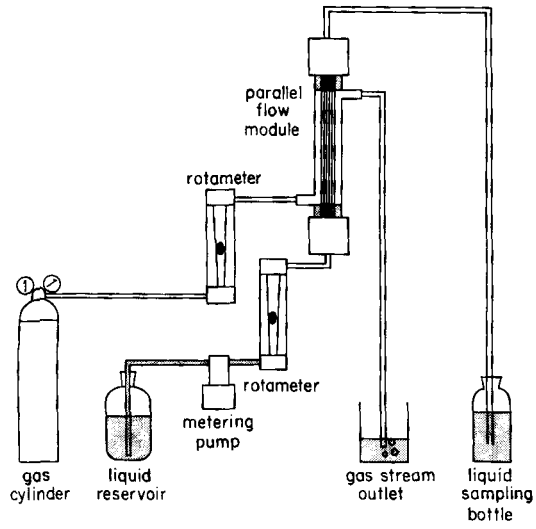

Figure 2. Experimental apparatus.

The overall mass transfer coefficient K was collected by the following

$$K = \frac{-Q_L}{AH'} \ln\left[1 - H'\left(\frac{[O_2]_{in} - [O_2]_{out}}{[O_2^*]_{in} - [O_2]_{in}}\right)\right] \tag{1}$$

where Q_L is the liquid flow rate; A is the interfacial area; $[O_2]_{in}$ and $[O_2]_{out}$ are the inlet and outlet oxygen concentrations in the liquid, respectively; and $[O_2^*]_{in}$ is the liquid concentration in equilibrium with the inlet gas concentration. The dimensionless group H' is defined as

$$H' \equiv \left(1 + \frac{Q_L}{Q_G H}\right) \tag{2}$$

where Q_G is the gas flow rate, and H is the equilibrium ratio of gas concentration to liquid concentration. In our experiments, $Q_G H$ was usually much greater than Q_L, so H' was essentially equal to one. For oxygen removal, the gas stream was essentially free of oxygen, so $[O_2^*]_{in}$ was zero. Equation 1 then simplified to

$$K = \frac{Q_L}{A} \ln\left(\frac{[O_2]_{in}}{[O_2]_{out}}\right) \tag{3}$$

For carbon dioxide absorption, the inlet liquid was free of carbon dioxide, so the analogous relation to Eq. 1 simplified to

$$K = \frac{-Q_L}{A} \ln\left(1 - \frac{[CO_2]_{out}}{[CO_2]_{in}^*}\right) \tag{4}$$

These equations, special cases of more general results derived earlier (Zhang and Cussler, 1985a,b,c), were used to find the overall mass transfer coefficients reported in the following section.

Results

We made three chief types of experiments in this work. First, we studied mass transfer in hollow-fiber modules whose fibers contained flowing water and whose shells contained either a vacuum or a nitrogen sweep gas. Second, we measured mass transfer in modules where the vacuum or sweep gas was inside the fibers and where the water flowed outside the fibers and parallel to the fiber axis. Third, we made similar measurements in modules where the vacuum or sweep gas was inside the fibers, but the water flowed outside the fibers in crossflow, perpendicular to the fiber axis. These three types of experiments are reported below.

Before we report these experiments, we can benefit from a brief review of how mass transfer occurs in these contactors (Cussler, 1984). This review is most easily couched in terms of oxygen removal from water. The mass transfer involves three sequential steps. First, the oxygen diffuses out of the water to the membrane surface. Second, it diffuses into the vapor-filled pores in the walls of the hydrophobic hollow fibers. Third, when the oxygen reaches the other wall of the fibers, it diffuses into the surrounding vacuum or the nitrogen sweep gas.

The flux j of oxygen in such a case is given by

$$j = K[O_2] \tag{5}$$

where $[O_2]$ is the concentration of oxygen in the bulk liquid and K is an overall mass transfer coefficient based on liquid concentrations. The quantity $(1/K)$, often called the total resistance to mass transfer, is given by

$$\frac{1}{K} = \frac{1}{k_L} + \frac{1}{k_M H} + \frac{1}{k_V H} \tag{6}$$

where k_L, k_M, and k_V are the individual mass transfer coefficients in the liquid, across the membrane, and in the gas, respectively; and H again is a Henry's law constant, the equilibrium concentration in the gas divided by that in the liquid.

In many cases, one of the individual mass transfer coefficients will be much smaller than the others, and hence dominate K. We can often tell which one is important by varying the flows of gas and liquid. The liquid coefficient usually increases with liquid fluid but is independent of gas flow. The membrane coefficient k_M varies with neither flow, but may dominate K when both liquid and gas flows become large. We will use these characteristics to analyze the behavior that follows.

When water flows inside the fibers, the mass transfer coefficients for oxygen vary with water flow but not with gas flow, implying that k_V does not contribute significantly to K. Moreover, the data show no evidence of reaching an asymptotic value at large water flow, suggesting that k_M is not important over the range studied. Thus when water flows inside the fibers, k_L seems to dominate K.

The idea that mass transfer in the water controls deaeration gains powerful support from the results in Figure 3. In this figure the logarithm of the mass transfer coefficient K, plotted as a Sherwood number, varies with the logarithm of water velocity per module length, plotted as a modified Peclet number. The 16-fiber modules (squares) were of different lengths but contained well-spaced fibers; in the 120-fiber modules (triangles) fiber spacing was random. The 2,100-fiber module (diamonds) had a volume fraction of 0.4. The solid line is a prediction based on the Sieder-Tate (1936) heat transfer correlation. The values of K for these modules of different geometries all fall along this line.

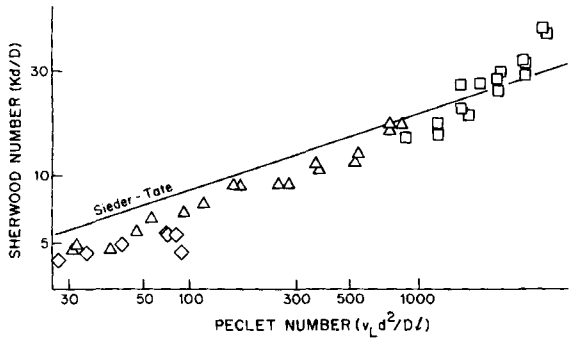

Figure 3. Mass transfer for water flowing through well-spaced fibers.

□ 16-fiber module, well-spaced
△ 120-fiber module, randomly spaced
◊ 2,100-fiber module, vol. frac. 0.4
— Prediction from Sieder-Tate (1936) heat transfer correlation

This occurs even though the volume fraction of fibers in the module varies from 3 to 30%. Of course, the flow within the fibers is unaltered by events in the fiber wall or outside the fibers, so k_L and hence K are similar in all modules.

These results imply that the key to oxygen mass transfer is diffusion in the liquid. For other solutes, the results may not be as simple. This is especially true when the mass transfer is accelerated by chemical reactions in the liquid. An example, shown in Figure 4, is carbon dioxide absorption with sodium hydroxide. The triangle and diamonds in this figure are for modules with 16 and 300 fibers, respectively. As in Figure 3, the liquid flows inside the fibers and gas flows outside. Now, however, the liquid is aqueous sodium hydroxide, which reacts rapidly with carbon dioxide in the gas outside. The rapid reaction accelerates mass transfer in the liquid, so that the membrane can limit the mass transfer at high flows. The data show that at equal Peclet number, the mass transfer coefficient is different in a well-spaced 16-fiber module than in a 300-fiber module. As the flow becomes very large, the mass transfer coefficients become equal. This equal value at high flow represents mass transfer across the membrane, which takes place too quickly to be seen when there is no chemical reaction.

Mass transfer in the liquid apparently also controls oxygen removal when the water flows outside of but parallel to the hollow fibers. This is shown in Figure 5, where the mass transfer coefficients of the 16- and 120-fiber modules (squares and triangles, respectively) fit the same correlation. As *in Figure 3*, the mass transfer coefficient K is incorporated in a Sherwood number and plotted vs. liquid velocity per module length written as a modified Peclet number. The close-packed 2,100-fiber module (diamonds) shows mass transfer independent of flow and over ten times slower than that in the 16-fiber module. Velocity is reported as a Reynolds number. The characteristic length in the Reynolds number is not the internal diameter of the hollow fiber, but an equivalent diameter d_e defined as

$$d_e = \left[\frac{4\,(\text{Cross-sectional area})}{\text{Wetted perimeter}}\right] \tag{7}$$

This quantity is often effective for heat transfer correlations.

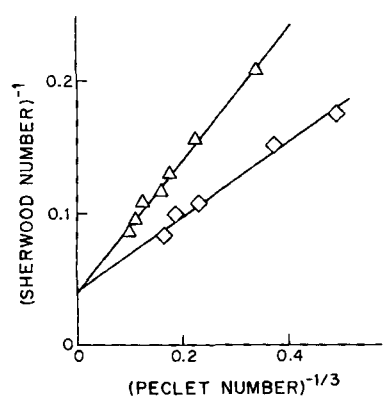

Figure 4. Carbon dioxide mass transfer into hollow fibers.

△ 16-fiber module
◊ 300-fiber module

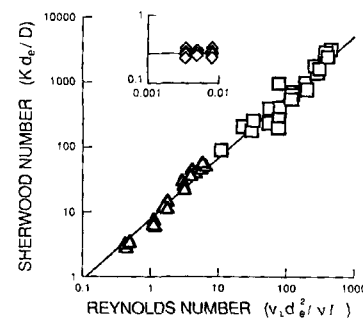

Figure 5. Mass transfer for water flowing outside and parallel to the hollow fibers.

□ 16-fiber module, well-spaced
△ 120-fiber module
◊ 2,100-fiber module, close-packed

However, when the fibers are closely packed, the mass transfer coefficient becomes independent of flow, as shown in the inset of Figure 5. Now the Sherwood number has a constant value of about 0.24. Under many circumstances we would interpret this as evidence that the membrane resistance has become important. In this case, we are not so sure. The membrane resistance almost certainly is not important for less densely packed fibers, so it seems strange that it is suddenly significant here. Instead, we suspect that there is major channelling through the closely packed fibers, and that the mass transfer is controlled by diffusion through nearly stagnant liquid trapped between the fibers, not by the membrane.

When water flows across beds of gas-filled hollow fibers, the oxygen mass transfer coefficients depend on liquid flow and module geometry as shown in Figure 6. The two upper data sets in the figure are for oxygen removal, the two lower sets are for carbon dioxide removal. Squares refer to a close-packed module with 750 fibers; triangles refer to modules with 72 well-spaced fibers. The lines shown are given only as visual aids; more detailed correclations are given in Table 2. The variation with liquid flow is similar for both widely spaced and close-packed modules. However, at equal flow, the mass transfer coefficients for widely spaced fibers are about 40% lower than those in closely spaced fibers. We suspect that this difference is the result of wakes formed downstream behind each fiber. When the fibers are sufficiently close that the wakes interact, mass transfer should be enhanced. These results are consistent with infer-

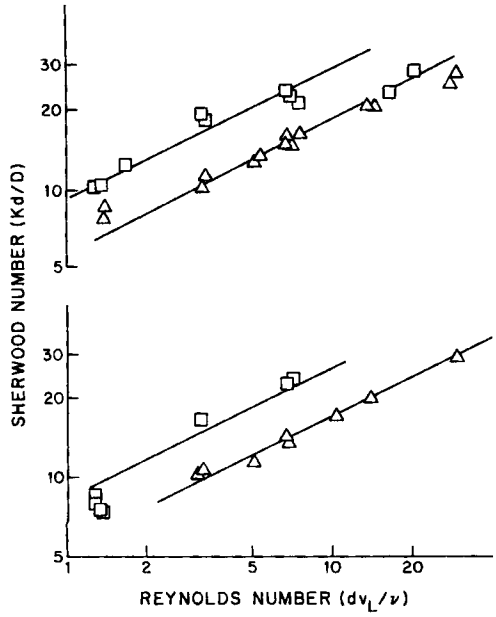

Figure 6. Mass transfer for water flowing across hollow fibers.

Top, O_2 removal; bottom, CO_2 removal
△ 72-fiber module, well-spaced
□ 750-fiber module, close-packed

ences of heat transfer experiments, as discussed in the next section.

Discussion

The results reported above strongly indicate that the performance of microporous hollow-fiber modules is almost always controlled by mass transfer in the liquid phase. The data in Figures 3, 5, and 6 are consistent with this conclusion. The exception occurs when liquid phase mass transfer is accelerated by chemical reaction and by very fast liquid flow, as shown in Figure 4.

The small membrane resistance observed is a consequence of the choice of a hydrophobic fiber. This fiber is not wet by the water, so its pores remain filled with gas. Diffusion through the gas is fast, making the membrane resistance unimportant. Indeed, the membrane material is unimportant, for any hydrophobic membrane of the same size should give the same results.

These conclusions would be different had we used a hydrophilic fiber. Then the fiber's pores would fill with water, and diffusion through the water would be much slower. The membrane's resistance would significantly retard the mass transfer. If the membrane's resistance becomes dominant, the configuration of the module would not matter, for all modules with the same membrane area would give the same mass transfer.

Because the membrane resistance is usually negligible in our experiments, the mass transfer reaches a maximum rate. In this section, we discuss two implications of this conclusion. First, we compare mass transfer correlations drawn from our data with those expected from the literature. Such a comparison is impor-

Table 2. Mass Transfer Correlations for Hollow-Fiber Modules*

Flow	Module	Ext. Void Frac.	Correlation** Observed†	Liteature‡	Remarks
Water inside	16-fiber	0.97	$Sh = 1.64\ Pe^{0.33}$	$Sh = 1.86\ Pe^{0.33}$[a]	Characteristic diameter d is that inside a fiber. The first literature correlation is empirical, the second is theoretical.
	120-fiber	0.74	—	$Sh = 1.62\ Pe^{0.33}$[b]	
	2,100-fiber	0.60	—	—	
Water outside in parallel flow	16-fiber	0.97	$Sh = 1.25\left(Re\frac{d_e}{\ell}\right)^{0.93} Sc^{0.33}$	$Sh = 0.022\ Re^{0.60} Sc^{0.33}$[c]	Characteristic diameter d is the equivalent value defined by Eq. 7. The correlation shown gives an unusually high Reynolds number dependence; other literature gives a smaller exponent.
	120-fiber	0.74	—	—	
	2,100-fiber	0.60	$Sh = 0.24$	—	
Water outside in cross flow	72-fiber	0.93	$Sh = 0.90\ Re^{0.40} Sc^{0.33}$	$Sh = 0.91\ Re^{0.39} Sc^{0.33}$ (single tube) $Sh = 0.32\ Re^{0.61} Sc^{0.33}$ (widely spaced tube bank)	Characteristic diameter is the external diameter of a fiber. Literature correlations for other tube spacings are similar to those given here.
	750-fiber	0.30	$Sh = 1.38\ Re^{0.34} Sc^{0.33}$	$Sh = 0.39\ Re^{0.59} Sc^{0.33}$ (closely spaced tube bank)	

*Correlations based on experiments with O_2, where there is no chemical reaction.
**Dimensionless groups are defined as follows:
Sherwood number $Sh = kd/D$
Peclet number $Pe = d^2v/D\ell$
Reynolds number $Re = dv/\nu$
Schmidt number $Sc = \nu/D$
†Based on a Schmidt number for O_2-H_2O of 476
‡From Kreith and Black (1980), except as indicated
(a) Sieder and Tate (1936)
(b) Leveque (1928)
(c) Knudsen and Katz (1958)

tant because it tests the reliability of the design equations that are the chief goal of this work. Second, we discuss the design of a particular device, the human gill. Such a gill will allow a human to breathe air dissolved in water, just as a fish does.

Mass transfer correlations

The mass transfer correlations developed in this work are compared in Table 2 with those published for related systems. The first column gives the nature of the water flow, the second and third columns characterize the hollow fiber module. The fourth column gives the mass transfer correlation found in this work. The mass transfer coefficient itself is reported as a Sherwood number $Sh(=Kd/D)$. The variations in water velocity and module length are reported as a Reynolds number $Re(=dv_L/\nu)$ or a modified Peclet number $Pe(=d^2v_L/D\ell)$. (This form of Peclet number is also called a Graetz number.) Note that the characteristic diameter d is not always defined in exactly the same way, as explained in the *Remarks* column of the table. Note also that the kinematic viscosity ν and the diffusion coefficient D have not been varied in our experiments. Their appearance in our correlations represents a hypothesis based on literature results.

The fifth column in Table 2 reviews correlations given in the literature. Like its antecedents, this fifth column is based on both idealism and ambiguity, for many partially conflicting correlations have been reported. We have tried to include those that seem most generally accepted. In so doing, we have omitted many that are familiar.

Table 2 shows that our results are very similar to those expected for flow within small tubes and to those for flow across small tubes. They are less similar to those for flow outside of but parallel to small tubes. Each of these three cases merits further discussion.

For flow through small tubes, our correlation is essentially identical with those reported earlier by Lévêque (1928) and by Sieder and Tate (1936). This identity is consistent with other earlier experiments, which also found that these literature correlations provide a sound basis for design. We suspect that errors in our experiments make it difficult to choose between these two. Still, we note that our results agree more exactly with the theory due to Lévêque than with the later empiricisms of Sieder and Tate. It may be that the latter correlation, based on heat transfer experiments, includes some free convection that augments the heat flux.

For cross flow around loosely packed fibers, our correlation is essentially identical with that expected from heat transfer from single tubes. Strictly speaking, this heat transfer result is valid only for Reynolds numbers between 4 and 40, which is roughly the range covered by our experiments. This close correspondence between our result and that in the literature makes us confident that related correlations for cross flow at other Reynolds numbers can be used with confidence to design different loosely packed modules.

Interestingly, our results for close-packed fibers also seem to agree with the results for single tubes. They do not agree as well with results for tube banks, even though the tube banks are more similar geometrically (Kreith and Black, 1980). We are not sure why this is so. The obvious rationalization, that our tubes are sufficiently separated to behave as single cylinders, is simply not true quantitatively, for the fibers are almost touching. Still, the conclusion is obvious: use single-tube correlations as a basis for new designs.

For parallel flow outside of hollow fibers, our results do not agree with scattered previous correlations for this unbaffled laminar flow. The mass transfer coefficients that we observe are larger and much more than expected from the Reynolds number. We can not explain these unexpected results. The obvious answer is some type of secondary flow. When we consulted heat transfer experts, they all volunteered this rationalization. However, these same experts could not suggest specific references that supported this idea. Even with secondary flows, most laminar flow correlations give a Reynolds number exponent of 0.5; turbulent flow correlations at Reynolds numbers well above those used here give an exponent of less than 0.8 (Kreith and Black, 1980).

Human gill

As an example of the use of these correlations, we turn to the design of a human gill. We choose this example because of its charm: while such a gill has a limited commercial value, it illustrates factors important to many designs using hollow fibers. To support a man, such a gill must supply up to 2,500 cm^3 of oxygen per minute. It must do so with an oxygen concentration in the lung about two-thirds that at sea level. This means a partial pressure around 100 mm Hg (13.3 kPa), which is that on a 3,000 m mountain. The gill must discharge about the same amount of carbon dioxide under a similar driving force. This can cause major problems in gills based on membranes of polymers like silicone rubber, which have low CO_2 permeability. However, the mass transfer coefficients of oxygen and carbon dioxide in our modules are similar, so we will discuss only oxygen transfer here.

To design the gill, we must first decide on the geometry for the hollow-fiber module. We assume that water flows through the module at 10 cm/s, and that the diffusion coefficient of oxygen in this water is 2.1 10^{-5} cm^2/s. We then can calculate the mass transfer coefficient. For a module with 10 vol. % of commercially available 0.01 cm fibers, we find for cross flow that

$$k_L = 1.38\frac{D}{d}\left(\frac{dv_L}{\nu}\right)^{0.34}\left(\frac{\nu}{D}\right)^{0.33} = 1.38\frac{2.10^{-5}\,\text{cm}^2/\text{s}}{0.01\,\text{cm}} \cdot \left(\frac{(0.01\,\text{cm})(10\,\text{cm/s})}{0.01\,\text{cm}^2/\text{s}}\right)^{0.34}\left(\frac{0.01\,\text{cm}^2/\text{s}}{2.10^{-5}\,\text{cm}^2/\text{s}}\right)^{0.33} = 0.05\ \text{cm/s} \quad (8)$$

Similar calculations give values for k_L of 0.005 cm/s for flow inside the fibers of a 15 cm long module and of 0.01 cm/s for parallel flow outside the fibers of a 15 cm module. We will base further calculations on the cross-flow module because its mass transfer is the fastest.

We can now calculate the size required for the human gill from the following relation

$$J = kaV\Delta[O_2] \quad (9)$$

As mentioned above, J is 2,500 cm^3 of oxygen per minute, or 1.9×10^{-3} mol/s. The oxygen concentration difference is two-thirds the saturation value in water, which is 1.8×10^{-6} mol/cm^3. The area per volume in a module containing 10% of 0.01

cm fibers built like those used here has an area per volume a of 40 cm^2/cm^3. Thus

$$1.9 \times 10^{-3} \frac{\text{mol}}{\text{s}} = 0.05 \frac{\text{cm}}{\text{s}} \left(\frac{40\ \text{cm}^2}{\text{cm}^3}\right) V \left(\frac{2}{3}\right) 1.8 \times 10^{-6} \frac{\text{mol}}{\text{cm}^3}$$

$$V = 800\ \text{cm}^3 \tag{10}$$

The gill need only have a volume of hollow fibers equal to less than about one liter of milk.

Now there are approximations in this analysis that will make many blanch. Certainly, oxygen demand may be higher, or allowable oxygen concentration differences may be lower. The surrounding water may not be saturated with air, or may contain suspended material that fouls the fibers. Still, the numbers that we have used are almost identical with those used by others who have built successful small gills for canaries, gophers, or bullfrogs (Robb, 1965; Dibelius et al., 1965; Paganelli et al., 1967; Kawaguchi and Kuwana, 1985).

Other approximations are more serious. We have not considered loss of nitrogen from the lungs, which will occur if the gill is used for anything but very shallow diving (Paganelli et al.). Fish avoid this problem by filling their gills with blood, an unattractive option for human divers. We have not considered the work required to move the water through the gill, work that will almost certainly require a pump. Building a fiber module without such a pump is a much more challenging engineering design, one that both entices and frightens us. On the other hand, we were delighted to discover that nature has again anticipated us: the insect called the water boatman dives using a small hollow-fiber hair bundle as a gill (Paganelli et al., 1967; Rahn and Paganelli, 1968).

The key point in our analysis is that the mass transfer per volume in hollow-fiber modules is very fast. It is fast enough to make a compact human gill possible, if not practical. We look forward to learning how this fast mass transfer can be exploited by using the design equations reported in this paper.

Acknowledgment

This work was principally supported by the Celanese Corporation. Other significant support came from the National Science Foundation, Grant No. CPE 84-08999, and from the BOC group.

Notation

a = interfacial area per volume
A = interfacial area
$[CO_2]$ = carbon dioxide concentration
d = fiber diameter
d_e = equivalent diameter, Eq. 7
D = diffusion coefficient
H = Henry's law constant
H' = dimensionless group, Eq. 2
j = diffusion flux, mol/L^2t
J = total diffusion flux, mol/t
k_L, k_M, k_V = individual mass transfer coefficients in liquid, membrane, and gas, respectively
K = overall mass transfer coefficient
l = fiber length
$[O_2]$ = oxygen concentration
Q_L, Q_V = volumetric flows of liquid and gas, respectively
v_L = liquid velocity
V = module volume
ν = kinematic viscosity

Literature cited

Astarita, G., D. W. Savage, and A. Bisio, *Gas Treating with Chemical Solvents*, Wiley, New York (1983).
Cussler, E. L., *Diffusion*, Cambridge Univ. Press, London (1984).
Dibelius, N. R., A. Dounoucos, and W. L. Robb, "Permselective Membrane Systems for Underwater Life Support," 6th Ann. Conv., Underwater Soc. Am. (Aug., 1965).
Kawaguchi, N., and J. Kuwana, "Silicon Rubber Makes Artificial Gills," *New Scientist*, **106**(1450), 24 (Apr. 4, 1985).
Kiani, A., R. R. Bhave, and K. K. Sirkar, "Solvent Extraction with Immobilized Interfaces in a Microporous Membrane," *J. Memb. Sci.*, **20**, 125 (1984).
Kim, B. M., "Process for Separation of Molybdenum from Tungsten Leachates," U.S. Pat. No. 4,443,414 (Apr. 17, 1984a).
———, "Membrane-based Solvent Extraction for Selective Removal and Recovery of Metals," *J. Memb. Sci.*, **21**, 5 (1984b).
Knudsen, J. G., and D. L. Katz, *Fluid Dynamics and Heat Transfer*, McGraw-Hill, New York (1958).
Kreith, F., and W. Z. Black, *Basic Heat Transfer*, Harper and Row, Cambridge (1980).
Lévêque, J. A., *Amm Mines*, **13**, 201, 305, 381 (1928).
Paganelli, C. V., N. Bateman, and H. Rahn, "Artificial Gills for Gas Exchange in Water," *Underwater Physiology*, C. J. Lambertsen, ed., Williams and Wilkins, Baltimore, 450 (1967).
Rahn, H., and C. V. Paganelli, "Gas Exchange in Gas Gills of Diving Insects," *Respiration Physiol.*, **5**, 145 (1968).
Robb, W. L., "Thin Silicone Membranes—Their Permeation Properties and Some Applications," *Gen. Elec. Co. Tech. Ser. Rep.* #65-C-031 (Oct., 1965).
Sieder, E. N., and G. E. Tate, "Heat Transfer and Pressure Drop of Liquids in Tubes," *Ind. Eng. Chem.*, **28**, 429 (1936).
Snell, F. D.,. and Hitton, C. L., eds., *Encyclopedia of Industrial Chemical Analysis*, Interscience, New York (1966).
Treybal, R. E., *Mass Transfer Operations*, 3rd ed., McGraw-Hill, New York (1980).
Yang, M. C., "Hollow-Fiber Gas Treating," Ph.D. Thesis, Univ. Minnesota (1986).
Zhang, Qi, and E. L. Cussler, "Microporous Hollow Fibers for Gas Absorption," *J. Memb. Sci.*, **23**, 321 (1985a).
———, "Bromine Recovery with Hollow-Fiber Gas Membranes," *J. Memb. Sci.*, **24**, 43 (1985b).
———, "Hollow-Fiber Gas Membranes," *AIChE J.*, **31**, 1548 (1985c).

Manuscript received Jan. 2, 1986, and revision received May 21, 1986.